

Change of Morphology in High Molecular Weight Polyethylene during Die Drawing

Y. W. LEE* and J. X. LI†

Department of Manufacturing Engineering, Hong Kong Polytechnic, Hung Hom, Kowloon, Hong Kong

SYNOPSIS

Deformed high molecular weight polyethylene (HMWPE) rod, produced by die drawing at 115°C, was cleaved longitudinally at liquid nitrogen temperature and the cleaved surface was etched using a permanganic etching technique. A series of etched surfaces of HMWPE sections with different draw ratios (from 1 to 13) were analyzed employing scanning electron microscopy (SEM). The change of crystalline structure in HMWPE during die drawing was observed. In undrawn HMWPE, the spherulites were made up of sheaflike lamellae and scattered within the amorphous phase. During die drawing in the first instance, the microscopically inhomogeneous deformation occurred and the spherulites aligned along the drawing direction. At a draw ratio of about 7, local melting occurred, the spherulites disintegrated, and the sheaflike lamellae oriented, followed by strain-induced recrystallization and the growth of the lamellae. Finally, at a draw ratio of about 12, the plastic deformation of the lamellae occurred and microfibrils were formed. © 1993 John Wiley & Sons, Inc.

INTRODUCTION

Semicrystalline polymers can be processed below their melting points and oriented preferentially; thereby, their strength and moduli in the orientation direction are improved drastically.¹⁻³ Although this characteristic response of semicrystalline polymers is often exploited in solid-phase polymeric processing such as tensile drawing,⁴ solid-state extrusion,⁵ and die drawing,⁶⁻⁸ it is not well understood. The strain-hardening response of semicrystalline polymers is usually accompanied by the transformation of initially isotropic melt-crystallized semicrystalline polymers into a fibrous structure.⁹⁻¹⁰ It is generally recognized that isotropic semicrystalline polymers become fibrous when they are drawn to yielding. But the process of the transformation during drawing is still not very clear. In the most commonly quoted

model suggested by Peterlin,¹¹⁻¹³ the process has been described on the basis of rotation of the lamellae, phase-transformation twinning, chain-tilting, slip, and final disintegration of the lamellae into small chain-folded blocks built into a "shish-kebab" structure of microfibrils. This model implies that the long period in the fibrous structure should be close to that in the undrawn materials. However, the fact is that for drawn polyethylene the long period is dependent on draw temperature,^{14,15} and in some cases, the small angle X-ray scattering long-period peak intensity decreases and even disappears, and this can be interpreted in several ways.^{16,17} Hendra et al. suggested that there was some sort of local melting and recrystallization to enrich Peterlin's model.¹⁸ However, these hypotheses have not been verified directly; the process of the transformation from spherulite to microfibril has not been observed directly for bulk specimens. The major bar to the resolution of this problem is the absence of a suitable method by which a qualified specimen can be prepared from the bulk semicrystalline polymers for direct observation.

Transmission electron microscopy has been employed to observe directly the morphological changes in thin films.^{19,20} Thin films, however, are generally

* To whom correspondence should be addressed at Newson International Ltd., Suite 816, Ocean Centre, 5 Canton Road, Tsimshatsui, Kowloon, Hong Kong.

† Present address: Materials Research Institute, South China University of Technology, Guangzhou, People's Republic of China.

subject to a different stress regime and might deform differently when compared with bulk specimens. In addition, since thermal conductivity of polymers is poor, the bulk might suffer from "heat build-up" due to its inability to disperse heat effectively during processing. For melt-crystallized polyethylene sheets, local melting has been probed by the neutron scattering technique.^{21,22} Therefore, it is believed that the mechanism of deformation in bulk specimens is different from that in thin films.

The development of the permanganic etching technique by Olley et al.²³ permits the direct observation of fine details of the lamellar morphology in various polyethylene and polypropylene bulk specimens²³⁻²⁵ in contrast to the extensive earlier studies on thin films. However, few articles have been concerned with direct observation of the evolution of crystalline structure in semicrystalline polymers during deformation.

This paper reports the results of direct observation of the crystalline structure for a drawn high molecular weight polyethylene (HMWPE) specimen prepared by the permanganic acid etching technique and shows the details of the transformation of crystalline structure from spherular to microfibrillar for HMWPE during die drawing up to a draw ratio of 13.

EXPERIMENTAL

1. Materials

The material investigated in this study was commercially available high molecular weight polyethylene rods manufactured in Taiwan using the melt extrusion process. The local supplier could indicate only that the average molecular weight of the material was about 50×10^4 . However, the density, melting point, and melt flow index were measured to be 0.948 g/cm³, 132–134°C, and 0.20 g/10 min, respectively. The rods were also heated to 130°C (very near to the melting point) and no recovery in the axial and transverse dimensions could be observed. It is known that the recovery of dimensions is normally due to the recoil of the oriented molecules.²⁶ This implies that the directionality of the rods due to extrusion was not significant.

2. Die Drawing

Die drawing was performed on an Instron 4301 Materials Testing Machine. The billet with a diameter of 25 mm was drawn through a conical die with 7.2 mm die exit at 25 mm/min draw speed. During

drawing, the temperature of the die, the billet, and the aluminum block were maintained at 115°C. When about a 100 mm length of billet had been drawn through the die, the drawing process was terminated and the billet was permitted to cool under tension. After the billet temperature had dropped to below 50°C, the tension was relieved and the billet was taken out. The undeformed, deformed, and drawn portions of the billet were used for morphological observation. The remnant of the billet and the drawn portion were cleaved longitudinally at liquid nitrogen temperature and the cleaved surfaces were treated with permanganic etchant and observed with a scanning electron microscope (SEM).

3. Surface Etching

The permanganic acid etching technique adopted in this work was close to that described by Phillips²⁷ but with some modifications. The etchant used was a solution of 0.5% (wt/wt) potassium permanganate in 95% sulfuric acid; the etching and washing processes were performed under an ultrasonic bath. In the first instance, the cleaved surface was etched at 28–32°C for 120 min in a 50 mL beaker containing 30 mL etchant and the etched specimen was washed with 30% sulfuric acid, 30% hydrogen peroxide, distilled water, and acetone successively as described by Olley et al.²³ Then, the etched specimen was immersed in 30% hydrogen peroxide at 4°C for 4 h. Finally, the etched surface was reetched twice at about 4°C and was re washed.

4. Scanning Electron Microscopy

The etched surface of the specimen was coated with a gold layer in a Polaron SEM Autocoating Unit E5200. Altogether, nine runs were used to coat the gold layer, and a coating period of 20 s was employed in each run to avoid any damage to the morphology of fine lamellae caused by coating. A sequence of sections on the treated surfaces in the remnant billet and the drawn portion were observed in a Cambridge S250 scanning electron microscope.

RESULTS

1. Morphology of the Undrawn Billet

Figure 1 shows the electron micrographs of the lightly etched surface in the undrawn billet, i.e., it was etched at 20°C for 2 h only. The undrawn billet has a typical spherulite structure,²⁸ as can be seen

in Figure 1 (A). The average sizes of the spherulites are about $40\ \mu\text{m}$, with a maximum size of about $60\ \mu\text{m}$ and a minimum of about $15\ \mu\text{m}$. The spherulites are scattered randomly. In some cases, when the cleaving plane had just passed through the core of a spherulite, the sheaflike structure^{25,29-31} of the spherulite can be seen as shown in Figure 1(B). The lamellae in the sheaf have a thickness of about $100\ \text{nm}$ and a length of $2-3\ \mu\text{m}$ [Fig. 1 (C) and (D)]. The lamellae appear in an S-shape and the main axes of the sheaflike lamellae seem to orient randomly. Figure 1 (C) also reveals the boundary areas between the spherulites in the undrawn billet. In these areas, the lamellae are relatively rare and much shorter than that in the sheaflike structure, the core of spherulites having a length of about $0.2-0.7\ \mu\text{m}$, but still maintaining a thickness of about $100\ \text{nm}$,

whereas in the core of the spherulite, the lamellae are stacked fairly compactly, as shown in Figure 1 (D).

2. Morphology of the Deformed Billet

This study addresses the evolution of crystalline phase morphology in HMWPE during die drawing. To expose the change of the spherulites and the lamellae at the same time, the cleaved surface of the deformed billet was first etched at room temperature and then immersed in 30% hydrogen peroxide and, finally, reetched at low temperature. Figure 2 indicates the locations of a series of portions observed on the treated surface along the drawing direction. Portion A is the region at which the deformation of the billet has just begun; at Portion B, the billet has

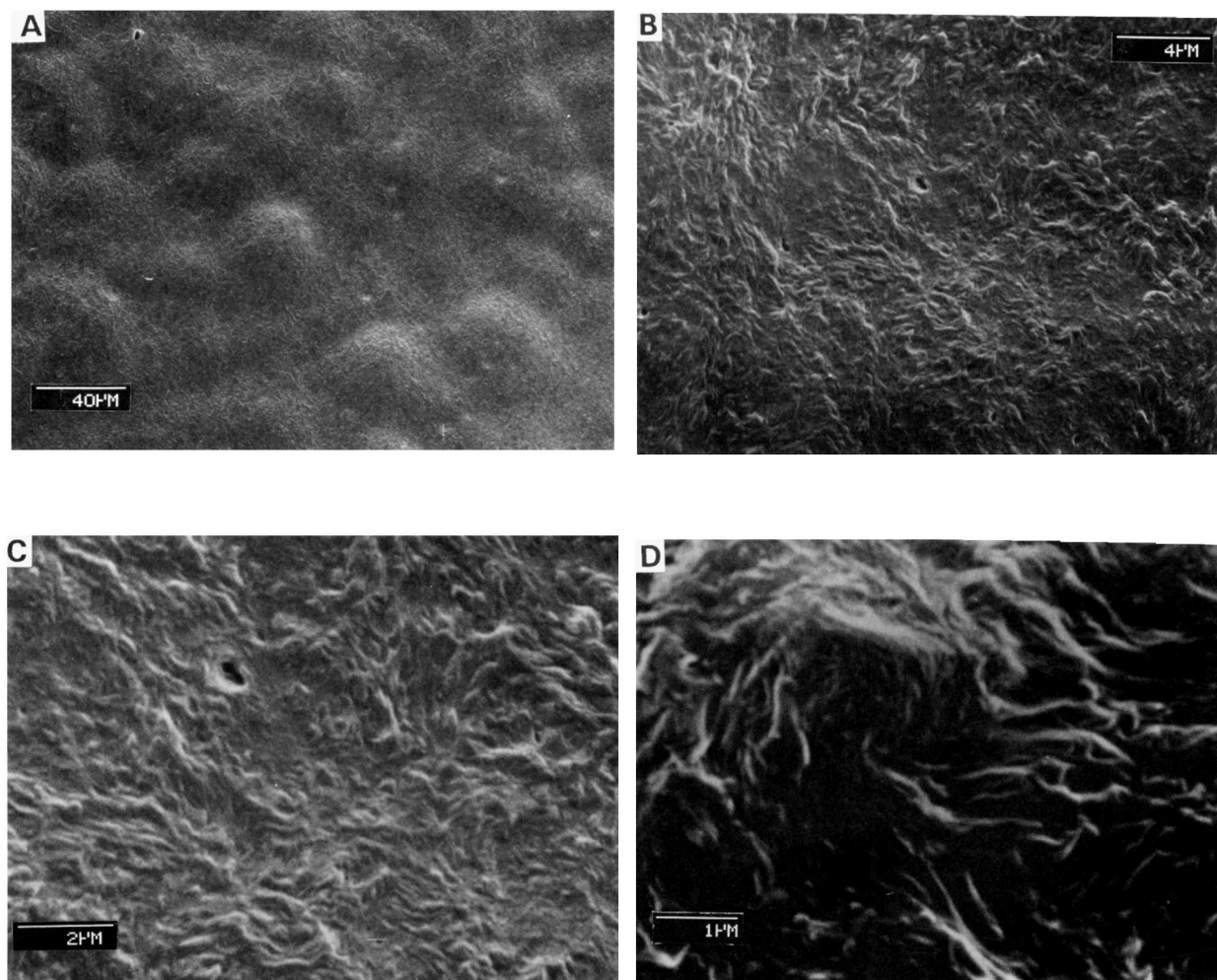


Figure 1 Electron micrographs of the undrawn HMWPE billet: (A) the spherulites in the undrawn billet; (B, C) the sheaflike lamellae in the spherulite; (D) a core of the spherulite.

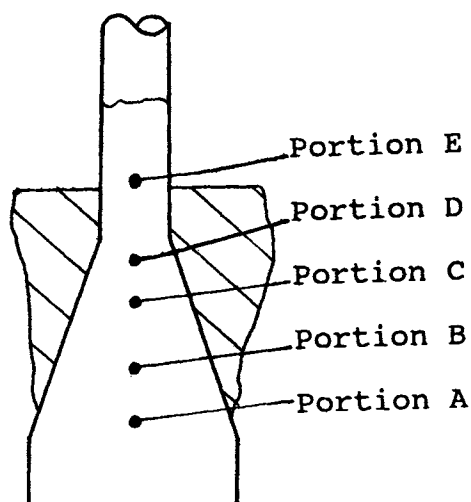


Figure 2 Location of the series of portions to be observed on the remnant of the billet.

been drawn to a draw ratio of 2; and at Portion C, the billet has reached the draw ratio of about 4 and begins to become transparent. At Portion D, the draw ratio of the billet is about 7; Portion E is at the exit of the die and the draw ratio is about 12.6.

Figure 3 shows an electron micrograph taken in Portion A. The morphology of the spherulite in this portion resembles that in the undrawn billet in size and distribution [refer to Fig. 1(A)] except that the boundary between the spherulites has been preferentially etched away. The spherulites with diameters ranging from 15 to 60 μm are also scattered ran-

domly. Actually, the deformation of the billet in this portion was slight; hence, the morphology of the spherulite should be similar to that in the undrawn billet.

Figure 4 shows the electron micrographs taken in Portion B, at which the billet had been drawn to a draw ratio of about 2. In this portion, the diameters of the spherulites still range from 15 to 60 μm , but the spherulites seem to have elongated along the drawing direction and have not deformed distinctly, as shown in Figure 4(A). Figure 4(B) shows an electron micrograph of the boundary areas between the spherulites. Compared to that in the undrawn billet [Fig. 1(C)], the lamellae between the spherulites seem to have increased in dimension and in quantity, and besides the lamellae, some small "spherulites" emerge, which have a size of about 0.7 μm . This may be the result of local melting during die drawing and then recrystallization during cooling. Although the spherulites in this portion start to align, the lamellae between the spherulites still orient randomly.

Figure 5 shows the electron micrographs taken in Portion C, at which the billet has been drawn to a draw ratio of about 4. In this portion, the spherulites have arranged in rows along the drawing direction [Fig. 5(A) and (B)]. The average dimension of the spherulites seems to decrease distinctly, i.e., the number of spherulites with smaller diameters has increased. Figure 5(C) shows an enlarged view of the texture between the spherulites. The texture shown in Figure 5(C) is rather different from that

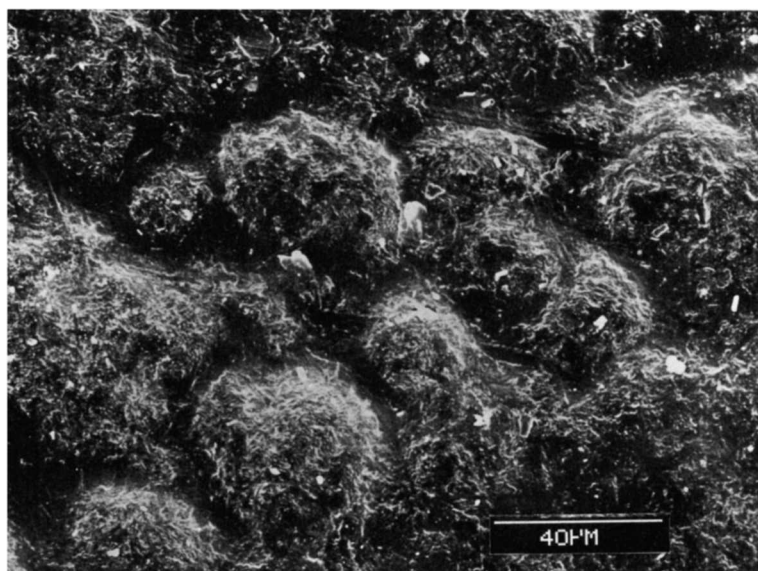


Figure 3 Electron micrograph of Portion A, which was deeply etched. The drawing direction is downward.

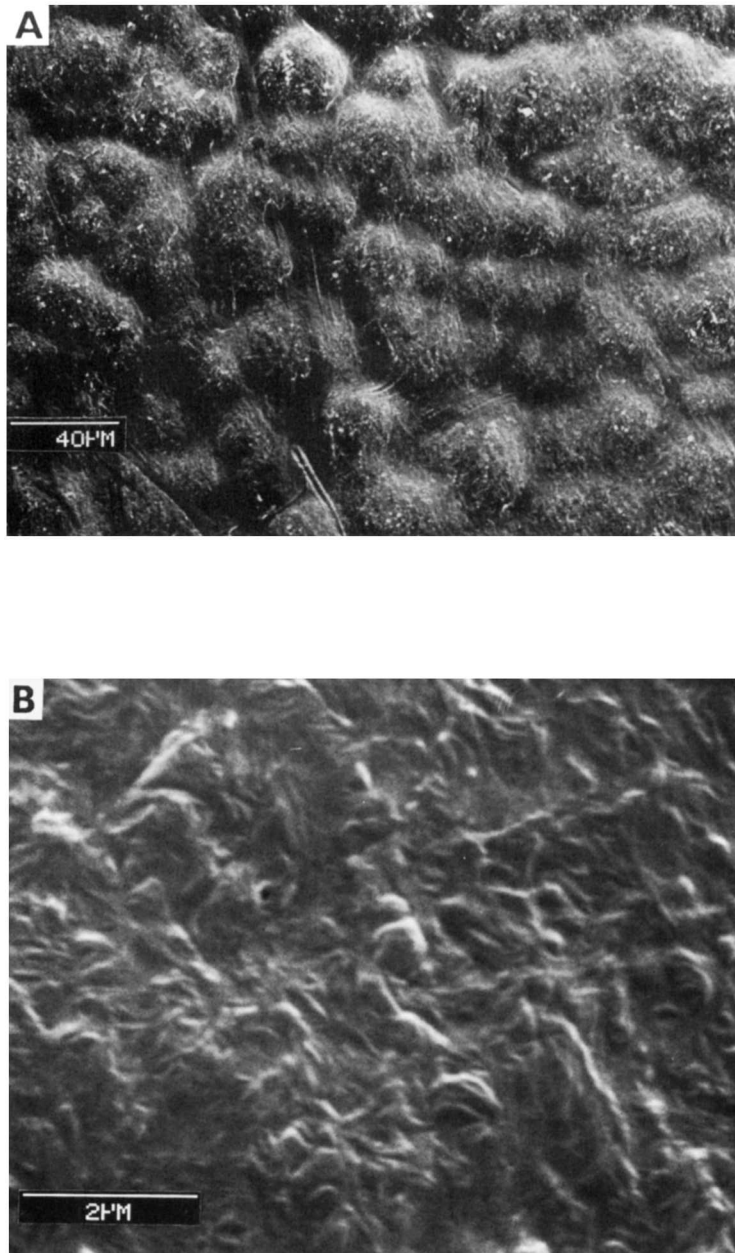


Figure 4 Electron micrographs of the deformed HMWPE billet at a draw ratio of 2. The drawing direction is downward. (A) Arrangement of the spherulites in the deformed billet; (B) the boundary area between the spherulites.

in Portion B [Fig. 4(B)]. In this portion, the lamellae are thicker and longer and the orientation of the S-shaped lamellae can be observed although there are still some unoriented lamellae that resemble those in Portion B [Fig. 4(B)]. This might be due to the disintegration of some small spherulites and the strain-induced crystallization during die drawing.

The morphology in Portion D is shown in Figure 6. This portion was situated near the neck of the die, at which the billet had been drawn to a draw ratio of about 7 and had become fairly transparent. In this portion, the structure of the crystal has changed substantially. Complete spherulites are now almost absent, and there are clear tracks of melt flow along the drawing direction [Fig. 6(A)]. Fur-

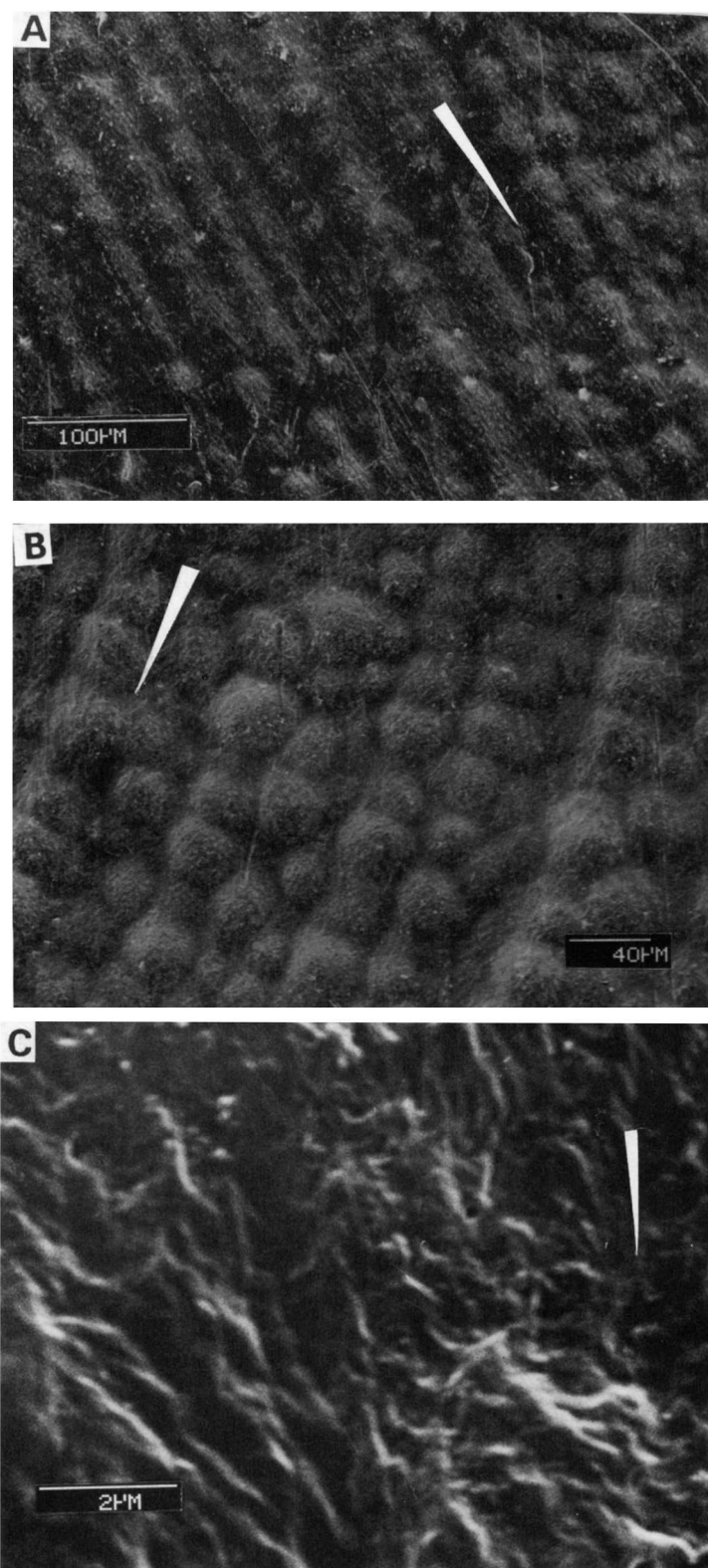


Figure 5 Electron micrographs of the deformed HMWPE billet at a draw ratio of 4. The draw direction is indicated by the arrow. (A, B) Arrangement in rows of the spherulites in the deformed billet; (C) the boundary area between the rows.

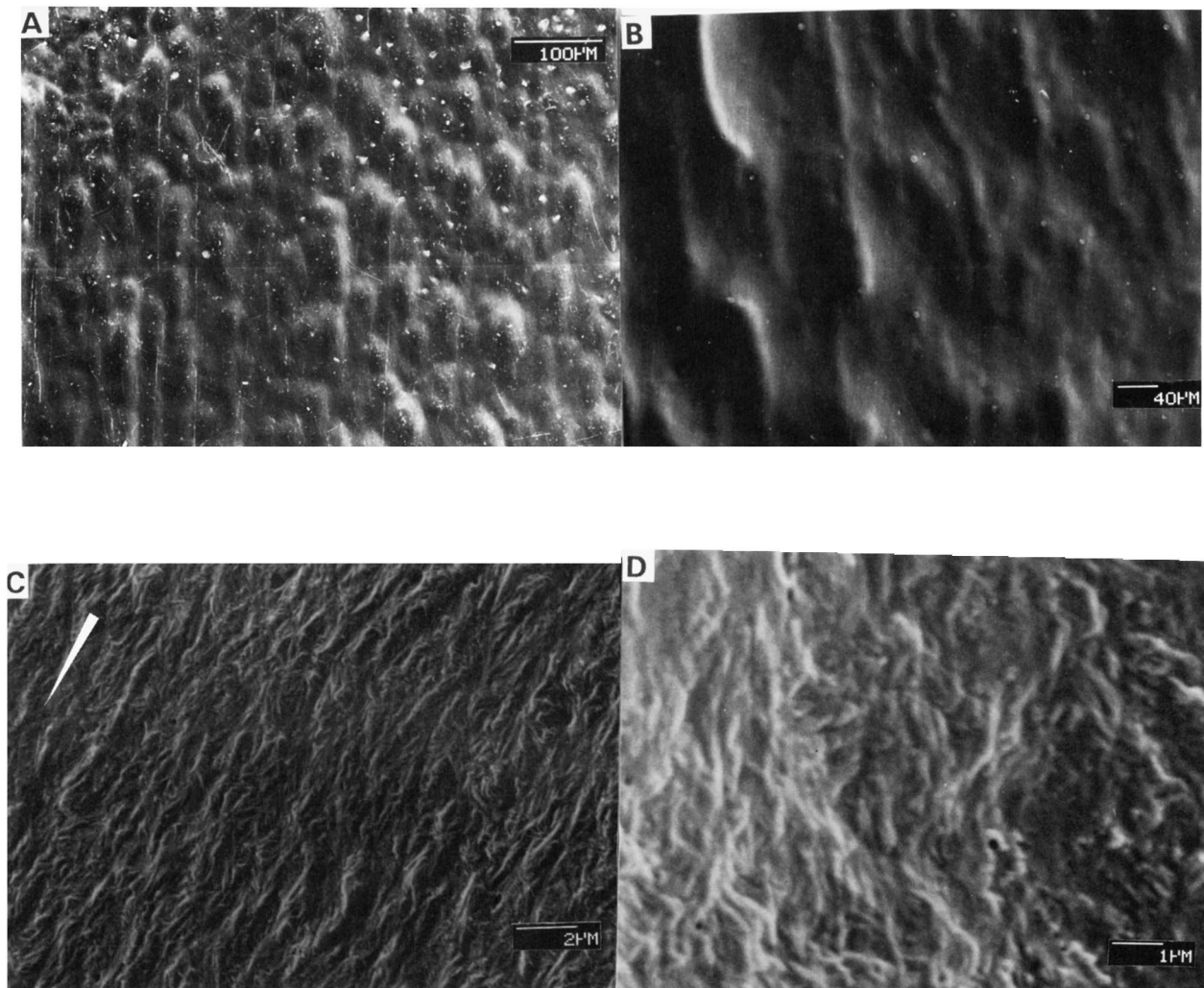


Figure 6 Electron micrographs of the deformed HMWPE billet at a draw ratio of about 7. The draw direction is downward. (A) The melt flow and disintegration of the spherulites in the deformed billet at a draw ratio of 6; (B) the disintegration of the spherulites in the billet at a draw ratio of 7.5; (C) an enlarged view of Figure 6(B), showing the oriented sheaflike lamellae; (D) details of the lamellae.

ther drawing results in the complete disappearance of the spherulites [Fig. 6(B)]. Figure 6(C) shows an enlarged detail of the morphology in Figure 6(B). When the billet has been drawn to this stage, the spherulites have completely disintegrated, leaving the S-shaped lamellae. Some of the lamellae coalesce laterally and form sheaf-lamellae, which are oriented in the drawing direction. Although the majority of the lamellae are oriented preferentially, there are some short lamellae lying randomly, as shown on the right side of Figure 6(D). Compared to that in the undrawn HMWPE, the lamellae become longer, thicker, and more compact. The lamellae can be as long as $5 \mu\text{m}$. Generally, the longer lamellae tend to

orient in the drawn direction. It is believed that this is the result of local melting and strain-induced crystallization.

Figure 7 shows the electron micrographs taken in Portion E, at which the billet had been just drawn out off the exit of the die and the draw ratio was approximately 12.5. In this portion, the morphology has developed further. Besides more oriented lamellae, a new category of structure emerges, which can be called "micella microfibrils" or the "embryo" of the microfibrils. These microfibrils are about 200 nm in width and still retain some degree of an S-shape. It is clear that they were formed by drawing the oriented lamellae in the sheaflike structure.

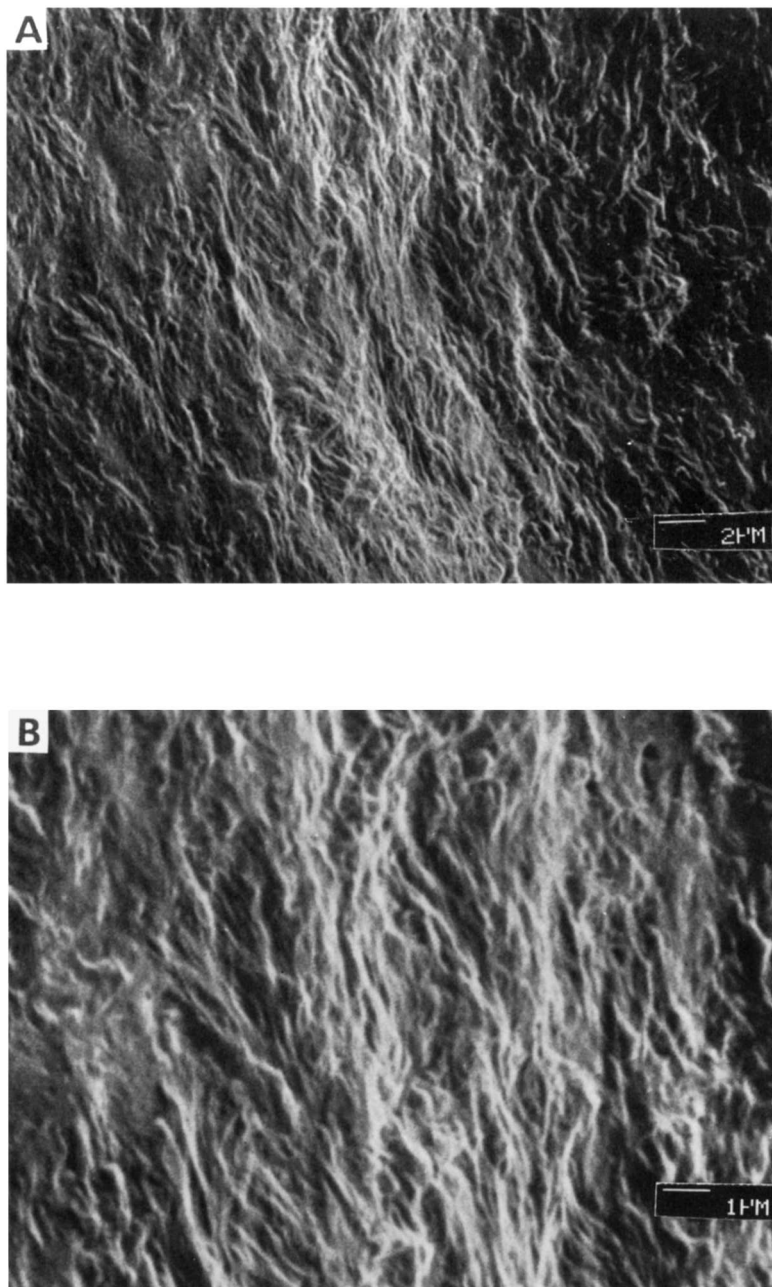


Figure 7 Electron micrographs of a drawn portion at the exit of the die with a draw ratio about 12.5, showing the micella microfibrils and the embryo of the microfibrils. The drawing direction is downward.

3. Morphology of the Drawn Products

Figure 8 is an electron micrograph of the drawn product, which has a draw ratio of about 12.6 and locates at a distance of about 100 mm from the exit of the die. Compared to that at the exit of the die (Portion E, in Fig. 7), the morphology has undergone a drastic change. The S-shaped lamellae have

vanished completely and the overall morphology is fibrous; but a few vestiges of S-shaped lamellae still remain; and the microfibril presents a little meandering. The diameters of microfibrils have been drawn to about 130 nm from 200 nm, as mentioned in the previous paragraph (refer to Fig. 7).

Figure 9 is the electron micrographs of the final product, which has a three-point bend modulus of

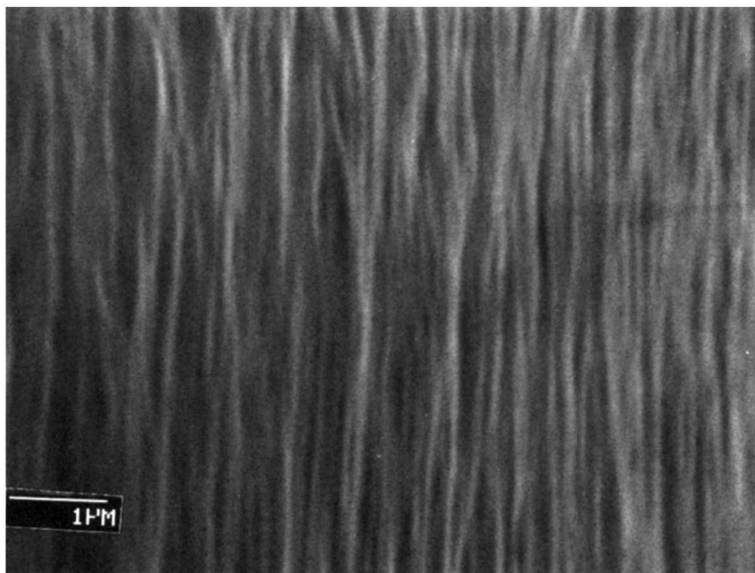


Figure 8 Electron micrographs of a drawn portion with a draw ratio of about 12.6 located at a distance of about 100 mm from the exit of the die. The drawing direction is downward.

about 16 GPa and is located at a distance of about 200 mm from the exit of the die. (The details of the determination of three-point bend modulus is discussed in another paper³²). The morphology of the final product appears to be very fibrous. The microfibrils have been drawn to a diameter of about 70 nm and extend straight along the drawing direction; they coalesce laterally and a few amorphous mate-

rials are embedded between them, whereas individual microfibrils appear to be structurally similar to needlelike crystals.

DISCUSSION

In this study, the sequence of micrographs has delineated the crystalline structure of HMWPE and

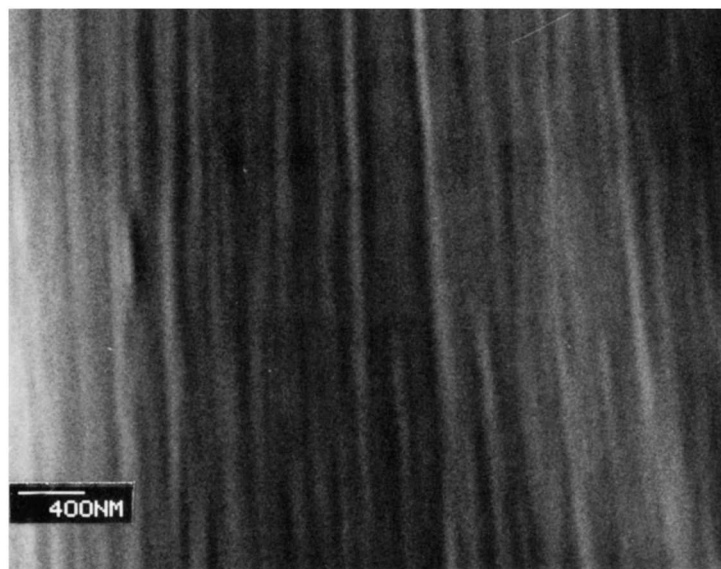


Figure 9 Electron micrographs of a drawn portion with a draw ratio of about 12.6 located at a distance of about 200 mm from the exit of the die. The drawing direction is downward.

their evolution from spherulite to microfibril during die drawing.

The process of deformation observed in this work is slightly different from that described by Peterlin. In Peterlin's model, the process of deformation is divided into three stages: the plastic deformation of spherulites, the transformation from spherulite to fibril, and the plastic deformation of the fibril. The transformation is envisaged as the breaking away of a small block of crystals from lamellar stacks in unoriented materials and subsequent reorientation and restacking to form microfibrils of oriented materials. However, in the present study, the plastic deformation of spherulites has not been identified; only the alignment of the spherulites at the low draw ratio and local melting and strain-induced recrystallization at the draw ratio of about 7 have been observed.

The crystalline structure in the final product is the laterally coalesced microfibrils, between which some noncrystalline amorphous materials are embedded. The "shish-kebab" structure, alternating amorphous and crystalline layers, which is considered as the characteristic structure of the microfibril,^{17,31} has not been observed. This may be due to the limitation of amplification for direct observation of specimens by SEM or the fact that the microfibril is a continuous crystalline phase that was formed by a strain-induced recrystallization. The latter may be true because for the drawn PE the SAXS long-period intensity decreases and even disappears when the draw ratio exceeds 10,^{16,17} which just corresponds to the process of the formation of microfibrils observed in this study (Figs. 6 and 7).

CONCLUSION

The crystalline structure of the undrawn HMWPE billet is a typical spherulitic structure that is made up of sheaflike lamellae scattered among the amorphous material. During die drawing, the crystalline structure changes as follows:

1. plastic deformation of interspherulite materials and alignment of spherulites;
2. local melting, disintegration of spherulites, and orientation of sheaflike lamellae;
3. strain-induced crystallization and growth of lamellae; and
4. plastic deformation of S-shaped lamellae and

formation of microfibrils by drawing the lamellae.

The crystalline structure of final drawn products consists of laterally coalesced microfibrils, between which some amorphous materials are embedded.

The authors would like to thank Mrs. Sni-ling Wong, Department of Applied Physics of Hong Kong Polytechnic, for assisting in preparation of the SEM micrographs.

REFERENCES

1. D. M. Bigg, *Polym. Eng. Sci.*, **28**, 830 (1988).
2. A. Peterlin, *Colloid Polym. Sci.*, **265**, 357 (1987).
3. L. H. Wang and R. S. Porter, *Polym. Commun.*, **31**, 457 (1990).
4. W. H. Carothers and J. W. Hill, *J. Am. Chem. Soc.*, **54**, 1566, 1579 (1932).
5. S. Kojima and R. S. Porter, *J. Polym. Sci. Polym. Phys. Ed.*, **16**, 1729 (1978).
6. I. M. Ward and P. D. Coates, *Polymer*, **20**, 1553 (1979).
7. A. K. Taraiya, A. Richardson, and I. M. Ward, *J. Appl. Polym.*, **33**, 2559 (1987).
8. A. Selwood, B. Parsons, and I. M. Ward, *Plast. Rubber Proc. Appl.*, **4**, 229 (1989).
9. J. Steidl and Z. Pelzbauer, *J. Polym. Sci. Part C*, 345 (1972).
10. A. G. Gibson, I. M. Ward, B. N. Cole, and B. Parsons, *J. Mater. Sci.*, **9**, 1193 (1971).
11. A. Peterlin, *J. Mater. Sci.*, **6**, 490 (1971).
12. A. Peterlin, *J. Polym. Sci. (C)*, **9**, 61 (1965).
13. A. Peterlin, *J. Polym. Sci. (C)*, **15**, 427 (1966).
14. A. Peterlin and F. Balta-Calleja, *J. Colloid Polym. Sci.*, **242**, 1093 (1970).
15. C. J. Farrell and A. Keller, *J. Mater. Sci.*, **12**, 966 (1977).
16. W. W. Adams, R. M. Briber, E. S. Sherman, R. S. Porter, and E. L. Thomas, *Polymer*, **26**, 7 (1985).
17. W. W. Adams, D. Yang, and E. L. Thomas, *J. Mater. Sci.*, **21**, 2239 (1986).
18. P. J. Hendra, H. William, and M. Taylor, *Polymer*, **26**, 1501 (1985).
19. P. M. Tarin and E. L. Thomas, *Polym. Eng. Sci.*, **19**, 1017 (1979).
20. P. M. Tarin and E. L. Thomas, *Polym. Eng. Sci.*, **18**, 472 (1978).
21. D. M. Sadler and P. J. Barham, *Polymer*, **31**, 36 (1990).
22. D. M. Sadler and P. J. Barham, *Polymer*, **31**, 43 (1990).
23. R. H. Olley, A. M. Hodge, and D. C. Bassett, *J. Polym. Sci. Polym. Phys. Ed.*, **17**, 627m (1979).

24. R. M. Gohil and P. J. Phillips, *Polymer*, **27**, 1687 (1986).
25. P. J. Phillips and R. J. Philot, *Polym. Commun.*, **27**, 307 (1986).
26. Y. W. Lee and S. H. Kung, *J. Appl. Polym. Sci.*, **46**(1) 9-18 (1992).
27. D. R. Norton and A. Keller, *J. Mater. Sci.*, **19**, 447 (1984).
28. P. E. Reed and G. Q. Zhao, *J. Mater. Sci.*, **17**, 3327 (1982).
29. K. L. Naylor and P. J. Phillips, *J. Polym. Sci. Polym. Phys. Ed.*, **21**, 2011 (1983).
30. N. V. Bhat, R. J. Howe, and D. M. Shinozaki, *J. Polym. Mater.*, **7**, 41 (1990).
31. D. R. Noyton and A. Keller, *Polymer*, **26**, 704 (1985).
32. Y. W. Lee and J. X. Li, to appear.
33. D. C. Bassett, *Principles of Polymer Morphology*, Cambridge University Press, Cambridge, 1981.

Received May 13, 1992

Accepted October 6, 1992